Magnetic force microscopy characterization of cobalt nanoparticles: A preliminary study

Livia Angeloni, Daniele Passeri, Pier Giorgio Schiavi, Francesca Pagnanelli, and Marco Rossi

View Online

Export Citation

ARTICLES YOU MAY BE INTERESTED IN

Magnetic Force Microscopy Characterization of Cobalt Nanoparticles: A Preliminary Study

Livia Angeloni[1], Daniele Passeri[1,2,a)], Pier Giorgio Schiavi[3], Francesca Pagnanelli[3] and Marco Rossi[1,2]

[1]*Department of Basic and Applied Sciences for Engineering, Sapienza University of Rome, Via A. Scarpa 14, 00161 Rome, Italy.*
[2]*Research Center for Nanotechnology applied to Engineering of Sapienza University of Rome (CNIS), Piazzale A. Moro 5, 00185 Rome, Italy*
[3]*Department of Chemistry, Sapienza University of Rome, P.le A. Moro 5, 00185 Rome, Italy*

[a)]Corresponding author: daniele.passeri@uniroma1.it

Abstract. In order to characterize magnetic properties of cobalt-based nanoparticles synthesized through electrodeposition on metal substrates, methods must be employed which enable the imaging of sample surface, the selection of a specific nanoparticle, and the accurate evaluation of local magnetic parameters, such as magnetic moment or saturation magnetization. Due to the combination of imaging capability and quantitative probing of ultra-low magnetic field through the use of a nanometer sized tip with a magnetic coating, magnetic force microscopy (MFM) is a promising tool to characterize Co-based nanoparticles directly on substrates. In this work, the report the preliminary results of the use of MFM to analyze Co nanoparticles electrodeposited on an Al substrate. The aim wa to assess the effective capability of this technique to investigate this kind of nanomaterials, foresee offered possibilities, and highlight current limitations to overcome.

INTRODUCTION

The broad range of applications of cobalt-based nanomaterials, from energy to sensors [1–4], requires the capability to control and tune geometrical and physical properties of the synthesized nanoparticles (NPs). In particular, among the different synthetic strategies, electrodeposition is particularly attractive when the direct synthesis of NPs on metal substrates is required [5]. Nevertheless, when using these deposition routes, methods for the physical characterization of NPs directly on the supporting substrates are required. As for the morphology, for instance, scanning electron microscopy (SEM) can be used to study size and numerical density of the NPs on the substrate, but more detailed information on the internal structure using transmission electron microscopy (TEM) cannot be retrieved due to difficulty to prepare the sample for TEM investigation. Characterization of physical and chemical properties can be an issue as well, as tools capable to visualize and probe the single NP on the surface are required. For example, the analysis of chemical composition may require the use of energy dispersive X-ray spectroscopy (EDX). Among the different physical parameters, the analysis of magnetic properties of Co-based NPs is difficult as standard tools like superconducting quantum interference devices (SQUID) [6], vibrating sample magnetometry (VSM) [7], or alternative gradient field magnetometry (AGFM) [8], generally enable the magnetic characterizations of a large number of NPs. Therefore, in order to characterize the magnetic properties of single Co NPs selected on the surface of the substrate, advanced techniques are required such as scanning magnetometry with Nitrogen-vacancy (N-V) color centers in diamond [9–13] or X-ray photoemission electron microscopy (XPEEM) [14, 15]. Although these methods allow accurate nanomagnetic characterizations with nanometer lateral resolution, they require not widespread experimental setups and thus these tools are not easily accessible for the broad scientific community. Conversely, magnetic force microscopy (MFM) is an atomic force microscopy (AFM) based technique generally included in most AFM standard setups, which are nowadays relatively widespread and thus easily accessible by the scientific community. MFM enables one to image the sample surface with nanometer lateral resolution, to selecte a specific location and thus a single NP, and to collect a signal which is proportional to the gradient of the tip-sample interaction force, and thus to probe the magnetic fields

produced by the sample, thanks to the use of a magnetically coated tip [16, 17]. Really, different techniques implementing MFM allowed to study different properties of different nanosystems based on magnetic NPs, e.g.: to detect the presence of magnetic NPs in polymers or biological matrices [18–23]; to study field-related magnetic phenomena in iron-oxide NPs [24, 25]; to quantitatively determine magnetic moment and saturation magnetization of iron oxide NPs [26–28]; to investigate superparamagnetic NPs [24, 29, 30]. Also, MFM was used to investigate Co [31] and CoPt [32] nanostructures and Co nanoclusters [33].

In this work, we report the results of a preliminary study we performed using MFM to analyze Co NPs electrodeposited on Al substrate, in order to verify the suitability of this technique for the quantitative characterization of this kind of nanomaterials, thus highlighting limitations to overcome and promising possibilities of the method.

MATERIALS AND METHODS

Nanoparticles synthesis

Electrodeposition of Co-based NPs was performed through a three-electrode jacketed glass cell, using an Al foil as working electrode (Alfa Aesar 99%, 0.25 mm thickness) with surface equal to 0.5 cm^2 and a 2.5 × 2.5 cm cobalt foil as counter electrode. An Ag/AgCl saturated electrode was used as reference electrode. Al electrode was etched for 10 minutes in 1 M NaOH to remove the native oxide layer on the surface prior to the electrodeposition, and then was immersed for 15 minutes in 1 M HNO$_3$ to smooth the surface. CoSO$_4$ · 7H$_2$O was dissolved in order to obtain a Co^{2+} concentration equal to 0.1 M. Na$_2$SO$_4$ 0.1 M and H$_3$BO$_3$ 0.5 M were employed as supporting electrolyte and pH buffer, respectively. During electrodeposition the pH could increase due to the simultaneous co-reduction of water and protons. A constant electrolyte temperature of 25 ± 0.1°C was maintained in all the experiments by using a circulating thermostat. Potentiostatic electrodeposition of Co NPs was performed by maintaining the working electrode at a constant potential value of -1.65 V respect Ag/AgCl until the overall transferred charge reached 20 mC.

Magnetic force microscopy

Magnetic force microscopy (MFM) characterization was performed using a standard AFM setup (Dimension Icon, Bruker Inc.) equipped with standard CoCr coated tips (MESP, Bruker Inc.), in air and at room temperature. In our experimental setup, the sample is placed on an electromagnet which can apply a magnetic field along the vertical direction, in both up and down direction, the intensity of which is sufficient to saturate the tip magnetization [34].

RESULTS AND DISCUSSION

Figure 1 shows an example of MFM characterization of an area of sample where 3 Co NPs are visible. Figure 1a reports the topography of the area obtained during the first scan of the area (the 'first pass') performed in tapping mode. Figure 1b shows the corresponding standard MFM phase image. MFM is a two-pass technique where, after the topographical profile of a line is acquired, the same line is scanned again at fixed lift height Δz and a magnetic signal is acquired [17], i.e., the phase shift $\Delta\varphi$ of the cantilever in our setup. Indeed, $\Delta\varphi$ depends on the gradient $\partial F_z/\partial z$ along the z direction perpendicular to the surface plane of the component along z of the long-range interaction force F_z through the relation

$$\Delta\varphi = -\frac{Q_c}{k_c}\frac{\partial F_z}{\partial z} \quad , \tag{1}$$

being Q_c and k_c the quality factor of the cantilever first resonance in air and the cantilever spring constant, respectively. When the tip is above the top of the selected NP, we assume a two-dipole model to describe the tip-NP interaction [35] and, thus, we describe the NP as a sphere with radius d uniformly magnetized with a magnetization M_{NP} and the tip as a punctiform magnetic moment m_{tip} located at a distance δ_{tip} from the tip apex [28]. Therefore, $\Delta\varphi$ is expressed by the relation

$$\Delta\varphi = \mu_0 m_{tip} M_{NP} \frac{Q_c}{k_c} \frac{d^3}{\left(\Delta z + d/2 + A_{sp} + \delta_{tip}\right)^5} \quad , \tag{2}$$

where μ_0 is the permeability of free space and A_{sp} is the first pass amplitude set-point [28, 36]. For the tips we used in this work, the producer supplies the value 1×10^{-13} emu for m_{tip}. In addition to the magnetic signal, nevertheless,
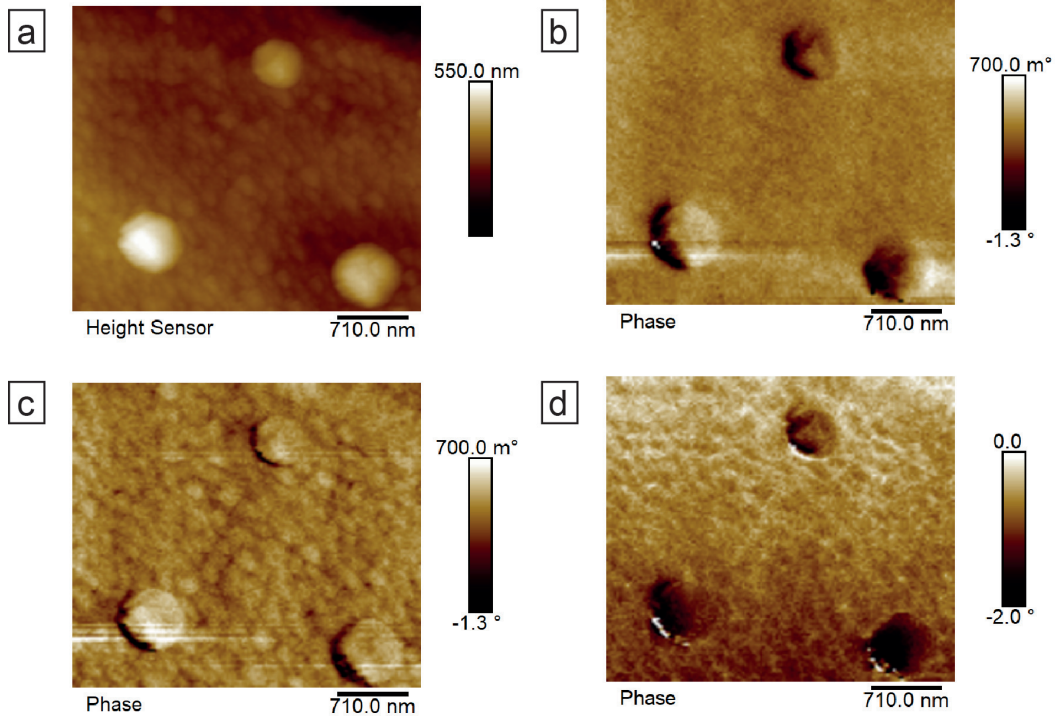
FIGURE 1. MFM analysis of an area of Al substrate with 3 Co NPs: (a) topography; (b) standard phase MFM image; (c) phase image obtained with the demagnetized tip; (d) magnetic image obtained after subtraction of image (c) from image (b).

standard MFM images are affected by tip-sample electrostatic forces given by

$$F_{el} = \frac{1}{2} V_{dc}^2 \frac{\partial C_{ts}}{\partial z} \quad , \tag{3}$$

where V_{dc} is the tip-sample static bias and C_{ts} is the tip-sample capacitance [37]. Therefore, modulation of the tip-sample bias and of the tip-sample capacitance result in electrostatic artifacts in MFM images [38–43]. In our method, electrostatic artifacts are removed by acquiring two subsequent images of the same area, the first in standard MFM and the second in MFM after demagnetization of the tip. More specifically, the sample is mounted on an electromagnet which can apply a magnetic field along the vertical axis [34]. The magnetization state of the tip is changed by applying and then switching off a magnetic field. By imaging the magnetic domains of a standard floppy disk, used as a reference material [44], the remanent magnetization of the tip is monitored and its remanent coercivity is determined [45]. Standard MFM image reflects both magnetic and electrostatic contributions, i.e.,

$$\Delta\varphi_{MFM} = \Delta\varphi_{magn} + \Delta\varphi_{el} \quad , \tag{4}$$

where $\Delta\varphi_{MFM}$ is the phase shift in standard MFM, $\Delta\varphi_{magn}$ is the phase shift due to only the tip-sample magnetic interaction, and $\Delta\varphi_{el}$ is the phase shift resulting from electrostatic forces. In the standard MFM phase image of the NPs reported in Fig. 1b, the contrast observed in correspondence of Co NPs cannot be easily rationalized on the basis of the simple two-dipole model. Indeed, while the smallest NP shows a roughly uniform dark contrast, indicating an attractive tip-sample force, the two biggest NPs appear partially dark and partially bright. In particular, as the scanning direction is from left to right, dark contrast is observed in correspondence of 'positive edges', i.e., in correspondence of the increase of the local height of the sample. Conversely, in correspondence of the decrease of the local height a bright contrast is observed. Such in-plane variation of the MFM contrast would suggest that the NPs have in-plane oriented magnetic domains. This nevertheless can be hardly justified as there are no sources of in-plane magnetic field, Co NPs were subject to the same vertical magnetic field used to magnetize the tip and, thus, an attractive interaction
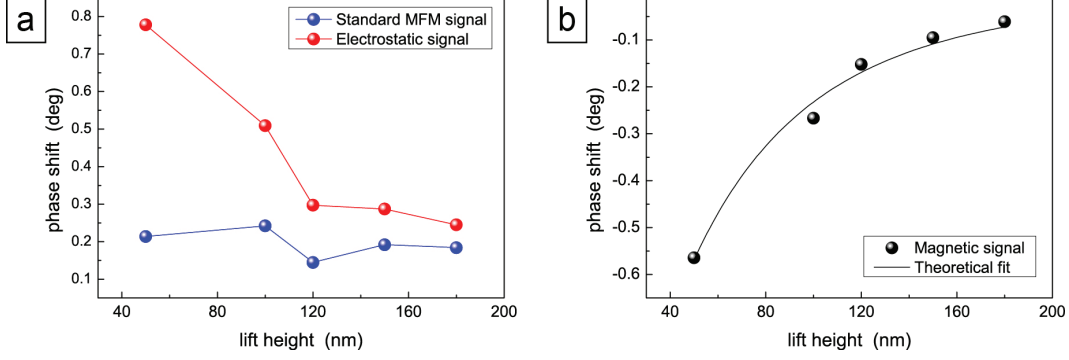
FIGURE 2. (a) Standard MFM phase shift (blue symbols) and electrostatic phase shift (red symbols) as a function of the lift height. (b) Pure magnetic phase shift as a function of the lift height (black symbols) and corresponding fit using the two-dipole model (solid line).

would be rather expected. Thus, Fig. 1b demonstrate that standard MFM is not suitable for magnetic imaging of Co NPs. In order to remove the effect of electrostatic forces, the corresponding phase signal is obtained by performing a second MFM image in the same experimental conditions except for the tip, which is demagnetized through the application of the remanent coercive field. Figure 1c shows such phase image obtained with the demagnetized tip. After demagnetization, only the electrostatic term $\Delta\varphi_{el}$ is present in the signal and, thus, contrast in Fig. 1c reflects only tip-sample nonmagnetic interaction. Therefore, by subtracting the two signals, $\Delta\varphi_{magn}$ is obtained, i.e., the pure tip-sample magnetic signal. Figure 1d shows the phase image after subtraction. Except for some noise in correspondence of the edges, NPs appear darker than the substrate, which indicates an attractive force between the tip and the NPs as expected, as during the magnetization of the tip the same magnetic field orientates the NPs and, thus, after switching off both tip and sample are at their remanent states with the magnetic dipoles aligned and oriented in the same direction. It is worth noting, however, that while the maximum applied field is sufficient to saturate the tip magnetization, there is the possibility that it could be not sufficient to saturate the magnetization of the NPs. Also, it must be noted that MFM is performed in absence of external magnetic field and, thus, Fig. 1d reflects the remanent magnetization of the NPs.

The presence of a neat magnetic attractive force demonstrates that the investigated NPs contain metallic Co and that, after electrostatic artifacts are removed, MFM can be effectively used to at least qualitatively detect the magnetic field generated by the NPs. In order to verify if MFM can be used also to quantitatively characterize magnetic properties of Co NPs, e.g., to determine their remanent magnetic moment and/or saturation magnetization, we selected an isolated NP the diameter of which was measured as high as $d = 150$ nm from topographical image, which is representative of the Co NPs observed on the sample. The difference between the phase values measured in correspondence of the top of the NP and of the substrate was measured as a function of the lift height Δz. Figure 2a shows the phase contrast versus lift height measured in standard MFM (blue symbols) in correspondence of the NP, obtained with the tip magnetized at its remanent saturation magnetization. Positive values of the $\Delta\varphi$ could be in principle indicate repulsive magnetic forces, which however would require that the magnetic moments of tip and NP are oriented in opposite directions, which could be not justifiable on the basis of our experimental setup. Also, the fact that standard MFM $\Delta\varphi$ is rather independent on Δz indicates that it is not the result of magnetic interaction. Indeed, when the tip is demagnetized by applying the tip remanent coercivity, the electrostatic phase shift reported in Fig. 2a (red symbols) is measured. The corresponding values of $\Delta\varphi$ are positive and decrease as Δz increases, as expected in the case of electrostatic interaction due to the modulation of the tip-sample capacitance [41]. This indicates that in our experiment electrostatic interactions are larger than magnetic ones [28, 45]. The difference between the two signals as a function of Δz, which is shown in Fig. 2b (black symbols), reflects the pure magnetic tip-sample interaction and is in good agrement with results previously observed on different kind of NPs and is well described by the two-dipole model. Therefore, in order to evaluate the remanent saturation magnetization of the NP, data reported in Fig. 2b can be fitted with Eq. (2). Assuming the magnetic moment of the tip equal to 1×10^{-13} emu as reported by the producer, the curve indicated with the solid line in Fig. 2b is obtained, allowing one to retrieve $A_{sp} + \delta_{tip} = 130 \pm 22$. As A_{sp} is about 30 nm, δ_{tip} is about 100 nm. Also, $M_{NP} = 15 \pm 6$ emu/g is found, which is significantly smaller than the saturation magnetization of Co NPs, as high as about 160 emu/g [46], but is compatible - or at least in the same order

of magnitude of - the remanent magnetization of Co NPs, reported as high as 60 emu/g [47]. This result is encouraging and demonstrates that MFM can be in principle suitable to quantitatively characterize magnetic properties of Co NPs, despite the approximations in the model we used. Nevertheless, there are currently several sources of uncertainty which must carefully considered. First of all, a certain variability of δ_{tip} as a function of the diameter of the analyzed NP is expected [48] and, therefore, in order to increase the significance of the method several NPs must be analyzed to obtain an accurate value of δ_{tip} [28]. Also, the diameter of the analyzed NP is significantly bigger than the tip radius and, therefore, it may be possible that the effective volume of material which contributes to the tip-sample magnetic interaction is smaller than the entire volume of the NP. As in Eq. (2) the NP is assumed uniformly magnetized, this would lead to the underestimation of M_{NP}. Future theoretical and simulative studies will be addressed to investigate the effective amount of sample generating the magnetic field probed by the MFM tip. Also, it must be noted that the remanent saturation magnetization of about 60 emu/g is obtained when the external magnetic field is enough intense to completely saturate NP the magnetization. Actually, we do not have evidences that the magnetic field we apply to magnetize the tip, i.e., 480 Oe, is sufficient to completely saturate the magnetization of the NP. This issue will be investigated in future studies. Another possible source of uncertainty is the value of m_{tip} we used for the calculation. Indeed, we used the value 1×10^{-13} emu supplied by the producer (without information about the uncertainty). Clearly, according to Eq. (2), a bigger value of m_{tip} results in a smaller calculated value of M_{NP}. For instance, in a previous work we calculated a value of 1.7×10^{-13} emu on the basis of several in-field magnetization curves of iron oxide NPs [28], which would results in the actual value $M_{NP} = 9 \pm 4$ emu/g. Notably, the procedure we used to evaluate m_{tip} cannot be applied in this case, and therefore, a different approach for the calibration of the tip magnetic moment must be designed. Finally, it must be observed that the electrodeposition route used in this work can easily lead to the presence of paramagnetic cobalt oxide and/or hydroxide at least on the surface of the NPs [49], thus reducing the apparent magnetization of the NP [47, 50, 51]. Therefore, also this issue must be addressed, for instance using the same MFM which can be used in principle to assess the presence of nonmagnetic material in magnetic NPs, e.g., in case of a coating on the magnetic core of the NPs [36].

CONCLUSION

In conclusion, the preliminary results reported in this work demonstrate the capability of MFM to characterize magnetic properties of Co-based NPs synthesized through electrodeposition on Al substrate. Really, due to the presence of electrostatic artifacts, standard MFM is not suitable for the nanomagnetic imaging of Co NPs and methods for the removal of electrostatic artifacts must be employed. As far as quantitative characterization of magnetic properties is concerned, the analysis of the phase shift in correspondence of a NP allowed us to determine a value of remanent magnetization saturation which is in the expected order of magnitude, but lower than values reported in literature. Presently, different sources of uncertainty have been identified, e.g., presence of oxide/hydroxide in or on the NPs, effective volume of the NP contributing to the probed signal, variability of the tip magnetic moment, which must be taken into account to perform accurate quantitative nanomagnetic characterization of Co-based NPs.

REFERENCES

[1]   P. G. Schiavi, L. Farina, P. Altimari, M. A. Navarra, R. Zanoni, S. Panero, and F. Pagnanelli, Electrochim. Acta **290**, 347–355 (2018).

[2]   P. G. Schiavi, L. Farina, R. Zanoni, P. Altimari, I. Cojocariu, A. Rubino, M. A. Navarra, S. Panero, and F. Pagnanelli, Electrochim. Acta **319**, 481–489 (2019).

[3]   P. G. Schiavi, L. Farina, A. Rubino, P. Altimari, M. A. Navarra, R. Zanoni, S. Panero, and F. Pagnanelli, AIP Conf. Proc. **2145**, p. 020012 (2019).

[4]   L. Wang, L. Xu, Y. Zhang, H. Yang, L. Miao, C. Peng, and Y. Song, ChemElectroChem **5**, 501–506 (2018).

[5]   P. G. Schiavi, P. Altimari, F. Pagnanelli, E. Moscardini, and T. L., Chemical Engineering Transactions **43**, 673–678 (2015).

[6]   M. M. Saari, K. Sakai, T. Kiwa, T. Sasayama, T. Yoshida, and K. Tsukada, J. Appl. Phys. **117**, p. 17B321 (2015).

[7]   J. Hu, I. M. C. Lo, and G. Chen, Sep. Purif. Technol. **56**, 249–256 (2007).

[8]   A. L. Urbano-Bojorge, N. Félix-González, T. Fernández, F. del Pozo-Guerrero, M. Ramos, and J. J. Serrano-Olmedo, J. Nano Res. **31**, 129–1375 (2015).

[9] C. L. Degen, Appl. Phys. Lett. **92**, p. 243111 (2008).

[10] L. T. Hall, J. H. Cole, C. D. Hill, and L. C. L. Hollenberg, Phys. Rev. Lett. **103**, p. 220802 (2009).

[11] A. Neumann, C. Thönnißen, A. Frauen, S. Heße, A. Meyer, and H. P. Oepen, Nano Lett. **13**, 2199–2203 (2013).

[12] S. Hong, M. S. Grinolds, L. M. Pham, D. Le Sage, L. Luan, R. L. Walsworth, and A. Yacoby, MRS Bull. **38**, 155–161 (2013).

[13] L. Rondin, J.-P. Tetienne, P. Spinicelli, C. Dal Savio, K. Karrai, G. Dantelle, A. Thiaville, S. Rohart, J.-F. Roch, and V. Jacques, Appl. Phys. Lett. **100**, p. 153118 (2012).

[14] F. Kronast, N. Friedenberger, K. Ollefs, S. Gliga, L. Tati-Bismaths, R. Thies, A. Ney, R. Weber, C. Hassel, F. M. Römer, A. V. Trunova, C. Wirtz, R. Hertel, H. A. Dürr, and M. Farle, Nano Lett. **11**, 1710–1715 (2011).

[15] O. Sandig, J. Herrero-Albillos, F. M. Römer, N. Friedenberger, J. Kurde, T. Noll, M. Farle, and F. Kronast, J. Electron Spectrosc. Relat. Phenom. **185**, 365–370 (2012).

[16] O. Kazakova, R. Puttock, C. Barton, H. Corte-León, M. Jaafar, V. Neu, and A. Asenjo, J. Appl. Phys. **125**, p. 060901 (2019).

[17] D. Passeri, L. Angeloni, M. Reggente, and M. Rossi, in *Magnetic characterization techniques for nanomaterials*, edited by C. S. S. R. Kumar (Springer-Verlag Berlin Heidelberg, 2017) Chap. 7,, pp. 209–259.

[18] C. Dong, S. Corsetti, D. Passeri, M. Rossi, M. Carafa, F. Pantanella, F. Rinaldi, C. Ingallina, A. Sorbo, and C. Marianecci, AIP Conf. Proc. **1667**, p. 020011 (2015).

[19] D. Passeri, C. Dong, M. Reggente, L. Angeloni, M. Barteri, F. A. Scaramuzzo, F. De Angelis, F. Marinelli, F. Antonelli, F. Rinaldi, C. Marianecci, M. Carafa, A. Sorbo, D. Sordi, I. W. C. E. Arends, and M. Rossi, Biomatter **4**, p. e29507 (2014).

[20] R. S. Silva, H. D. Mikhail, E. V. Guimarães, E. R. Gonçalves, N. F. Cano, and N. O. Dantas, Molecules **22**, p. 1142 (2017).

[21] M. Reggente, D. Passeri, L. Angeloni, F. A. Scaramuzzo, M. Barteri, F. De Angelis, I. Persiconi, M. E. De Stefano, and M. Rossi, Nanoscale **9**, 5671–5676 (2017).

[22] A. Krivcov, J. Schneider, T. Junkers, and H. Möbius, Phys. Stat. Sol. (a) **2018**, p. 1800753 (2018).

[23] L. Angeloni, M. Reggente, D. Passeri, M. Natali, and M. Rossi, WIREs Nanomed. Nanobiotechnol. **10**, p. e1521 (2018).

[24] C. Moya, O. Iglesias-Freire, X. Batlle, A. Labarta, and A. Asenjo, Nanoscale **7**, 17764–17770 (2015).

[25] C. Moya, Óscar Iglesias-Freire, N. Pérez, X. Batlle, A. Labarta, and A. Asenjo, Nanoscale **7**, 8110–8114 (2015).

[26] S. Sievers, K. F. Braun, D. Eberbeck, S. Gustafsson, E. Olsson, H. W. Schumacher, and U. Siegner, Small **8**, 2675–2679 (2012).

[27] X. Li, W. Lu, Y. Song, Y. Wang, A. Chen, B. Yan, S. Yoshimura, and H. Saito, Sci. Rep. **6**, p. 22467 (2020).

[28] L. Angeloni, D. Passeri, S. Corsetti, D. Peddis, D. Mantovani, and M. Rossi, Nanoscale **9**, 18000–18011 (2017).

[29] S. Schreiber, M. Savla, D. V. Pelekhov, D. F. Iscru, C. Selcu, P. C. Hammel, and G. Agarwal, Small **4**, 270–278 (2008).

[30] T. M. Nocera, J. Chen, C. B. Murray, and G. Agarwal, Nanotechnology **23**, p. 495704 (2012).

[31] H. S. Nagaraja, K. K. Nagaraja, F. Rossignol, F. Dumas-Bouchiat, C. Champeaux, and A. Catherinot, J. Supercond. Nov. Magn. **25**, 1901–1906 (2012).

[32] V. L. Mironov, B. A. Gribkov, S. N. Vdovichev, S. A. Gusev, A. A. Fraerman, O. L. Ermolaeva, A. B. Shubin, A. M. Alexeev, P. A. Zhdan, and C. Binns, J. Appl. Phys. **106**, p. 053911 (209).

[33] S. A. Koch, R. H. te Velde, G. Palasantzas, and J. T. M. De Hosson, Appl. Surf. Sci. **226**, 185–190 (2004).

[34] L. Angeloni, D. Passeri, M. Natali, M. Reggente, E. Anelli, A. Bettucci, D. Mantovani, and M. Rossi, AIP Conf. Proc. **1873**, p. 020008 (2017).

[35] U. Hartmann, Phys. Lett. A **137** (1989), 10.1016/0375-9601(89)90229-6.

[36] L. Angeloni, D. Passeri, F. A. Scaramuzzo, D. Di Iorio, M. Barteri, D. Mantovani, and M. Rossi, AIP Conf. Proc. **1749**, p. 020006 (2016).

[37] P. Girard, Nanotechnology **12**, 485–490 (2001).

[38] J. Yu, J. Ahner, and D. Weller, J. Appl. Phys. **96**, 494–497 (2004).

[39] C. S. Neves, P. Quaresma, P. V. Baptista, P. A. Carvalho, J. P. Araújo, E. Pereira, and P. Eaton, Nanotechnology **21**, p. 305706 (2010).

[40]   M. Jaafar, O. Iglesias-Freire, L. Serrano-Ramón, M. R. Ibarra, J. M. de Teresa, and A. Asenjo, Beilstein J. Nanotechnol. **2**, 552–560 (2011).

[41]   L. Angeloni, D. Passeri, M. Reggente, M. Rossi, D. Mantovani, L. Lazzaro, F. Nepi, F. De Angelis, and M. Barteri, AIP Conf. Proc. **1667**, p. 020010 (2015).

[42]   Y. Wang, Z. Wang, J. Liu, and L. Hou, Scanning **37**, 112–115 (2015).

[43]   M. Fuhrmann, A. Krivcov, A. Musyanovych, R. Thoelen, and H. Möius, Phys. Stat. Sol. (a) p. 1900828 (2020).

[44]   D. Passeri, C. Dong, L. Angeloni, F. Pantanella, T. Natalizi, F. Berlutti, C. Marianecci, F. Ciccarello, and M. Rossi, Ultramicroscopy **136**, 96–106 (2014).

[45]   L. Angeloni, D. Passeri, M. Reggente, D. Mantovani, and M. Rossi, Sci. Rep. **6**, p. 26293 (2016).

[46]   R. N. Grass and W. J. Stark, J. Mater. Chem. **16**, 1825–1830 (2006).

[47]   E. L. Dzidziguri, E. N. Sidorova, M. Inkar, A. G. Yudin, E. V. Kostitsyna, D. Y. Ozherelkov, K. V. Slusarsky, A. Y. Nalivaiko, and A. A. Gromov, Mater. Res. Express **6**, p. 105081 (2019).

[48]   C. Iacovita, J. Hurst, G. Manfredi, P. A. Hervieux, B. Donnio, J. L. Gallani, and M. V. Rastei, Nanoscale **12**, 1842–1851 (2020).

[49]   P. G. Schiavi, P. Altimari, R. Zanoni, and F. Pagnanelli, Electrochim. Acta **220**, 405–416 (2016).

[50]   Q. Yuanchun, Z. Yanbao, and W. Zhishen, Mater. Chem. Phys. **110**, 457–462 (2008).

[51]   A. S. Vijayanandan and R. M. Balakrishnan, Appl. Phys. A **126**, p. 234 (2020).